Intermolecular Electron Transfer by Quantum Mechanical Tunneling

Abstract. *The transfer of electrons from one molecule to another by quantum mechanical tunneling has recently been implicated in biological electron transport. This report describes observations of electron transfer between aromatic molecules in a rigid matrix, in which electrons apparently tunnel through tens of angstroms of inert solvent. The kinetics tend to confirm the tunneling process, which is likely to be an important means of electron transfer when diffusion is blocked by steric factors or immobilization of the reactants.*

Reactions in which trapped electrons apparently tunnel through tens of angstroms of inert solvent are now becoming well known (*1–3*). This report describes observations of electron transfer from one molecule to another:

$$\phi_2^- + \phi_3Et \longrightarrow \phi_2 + \phi_3Et^- \qquad (1)$$

where ϕ_2 is biphenyl and ϕ_3Et is triphenylethylene, which has a larger electron affinity than ϕ_2. The reaction was observed in rigid, glassy ethanol at 77°K. The ϕ_2^- and ϕ_3Et are separated, on the average, by tens of angstroms of solvent and are unable to diffuse. The radical anions ϕ_2^- and ϕ_3Et^- are well known (*4*) and have extinction coefficients greater than 10^4 at 407 nm (ϕ_2^-) and 514 nm (ϕ_3Et^-); thus it is easy to follow the progress of the reaction spectrophotometrically.

Long-range tunneling by electrons has also been reported in electron transfer in photosynthesis (*5*). It is quite conceivable that quantum mechanical tunneling is a pervasive factor in biological electron transport. It may also play a role in the chemical sensitization of living cells to radiation damage, which is important in the treatment of cancer. Tunnel transfer of electrons between molecules may be important in many situations where it has not been previously considered. The experiments described below may provide a technique by which intermolecular electron tunneling reactions can be studied in some detail.

Pulse radiolysis with ~13-Mev electrons from the Argonne linac produced ionization in the frozen matrix. Changes in the ϕ_2^- and ϕ_3Et^- concentrations were observed over the time range from 10^{-6} to 10^2 seconds after the application of ~10-nsec pulses of radiation as described previously (*6*). The separated charges produced by ionization are trapped in the matrix with an efficiency which gives about 2.5 trapped electrons per 100 ev of energy deposited by the radiation (*7*).

In this experiment the matrix always contained a high concentration (0.15*M*) of ϕ_2 and variable concentrations of ϕ_3Et (0.01*M* to 0.10*M*). Virtually all of the electrons were captured by these solutes. Since ϕ_2 was in excess, the predominant species produced was ϕ_2^-. The electrons are observed to transfer from ϕ_2^- to ϕ_3Et as a function of time. The decay of ϕ_2^- at 407 nm is shown in Fig. 1, and the growth of ϕ_3Et^- at 514 nm is shown in Fig. 2. The points in Figs. 1 and 2 represent experimental data; the lines in Fig. 1 represent simulations based on simple tunneling calculations (*2, 3, 6*).

Analysis of the data is slightly complicated by the fact that about 25 percent of the ϕ_2^- decays even in the absence of added ϕ_3Et. This is probably due to reactions of ϕ_2^- with positive charge and radicals formed by the radiation. In order to measure only the decay due to added ϕ_3Et, I plot (Fig. 1) the surviving fraction of the ϕ_2^-, A/A_0, that is, the ϕ_2^- absorbance (A) at each time divided by the absorbance (A_0) at the same time in a sample containing 0.15*M* ϕ_2 but no ϕ_3Et. Simple kinetic considerations show that the fractional method of plotting is the appropriate way to correct for the decay not due to added acceptor.

Corrections were also made for the absorbance of ϕ_3Et^- at 407 nm. At 407 nm the extinction coefficient of ϕ_3Et^- in ethanol glass is about 10 percent as large as the extinction coefficient of ϕ_2^-.

The reproducibility of the shapes of the decay curves was reasonably good, but the relative yields showed some fluctuation. Data for the ϕ_2^- decays were obtained in repeated experiments, and the yields are believed to be accurate to ± 5 percent. The data for the ϕ_3Et^- growths are believed to be accurate to ± 10 percent. The fractional growth of ϕ_3Et^- matches the ϕ_2^- decay within experimental error.

The samples were completely clear with no cloudiness, an indication that the molecules did not aggregate. The ϕ_2 and ϕ_3Et were apparently distributed homogeneously at the relatively high concentrations used here, since the ϕ_2^- and ϕ_3Et^- absorption bands were not shifted or split. Aggregation would be expected to cause marked changes in the spectra (*8*). Self-complexing of simple aromatic molecules, such as ϕ_2, appears to be rare or unknown (*9*). Even if there were aggregation, could the observed kinetics result? A rapid electron transfer ($<10^{-9}$ second) within the aggregate would seem more likely.

The simulated decay curves in Fig. 1 are in very good agreement with experiment. I calculated the simulated curves on the assumption that ϕ_2 and ϕ_3Et initially captured electrons in proportion to their concentrations, and that electrons captured by ϕ_2 could then transfer to ϕ_3Et by tunneling. It is thought that the electron must tunnel through an energy barrier, the height of which is equal to the energy which binds the electron to ϕ_2. The width of the barrier is the distance to the nearest ϕ_3Et. The cal-

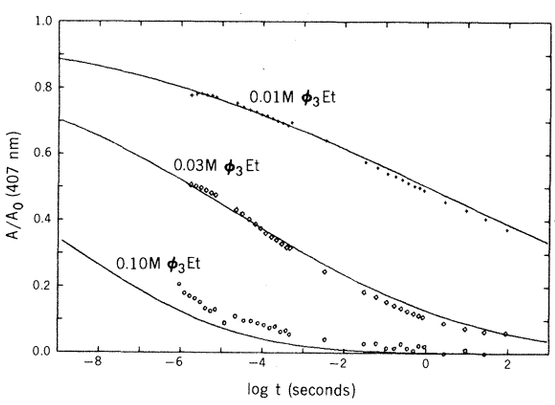

Fig. 1. Reaction of ϕ_2^- (ϕ_2 = 0.15*M*), observed at 407 nm, with ϕ_3Et in a rigid ethanol matrix at 77°K. The experimental points give the fraction of ϕ_2^- surviving (see text); the lines represent simulated decay curves based on simple tunneling calculations, which predict tunneling reaction distances of 18 Å at 10^{-6} second and 33 Å at 10^2 seconds. The experimental data are corrected for a small absorbance by ϕ_3Et^- at 407 nm.

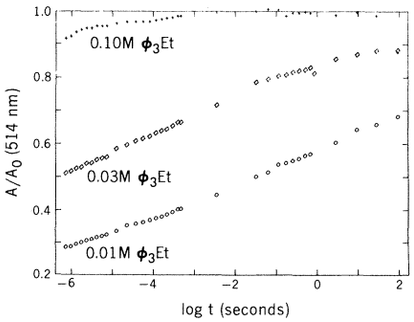

Fig. 2. Growth of ϕ_3Et^- absorbance (ϕ_2 = 0.15*M*) at 514 nm in a rigid ethanol matrix at 77°K. The fraction of electrons transferred from ϕ_2^- to ϕ_3Et is plotted by dividing the ϕ_3Et^- absorbance (A) by the absorbance (A_0) in 0.15*M* ϕ_3Et (without ϕ_2) at each point in time. In 0.15*M* ϕ_3Et all the electrons are initially captured by ϕ_3Et.

culation used to produce the simulations is little more than a rearrangement of a simple quantum mechanical formula. It gives the distance (in angstroms) at which a tunneling reaction may occur within time t (in seconds) (*2, 3, 6*) as:

$$a = a_0 + 2.26(15 + \log t)\, B^{-1/2} \quad (2)$$

where B is the binding energy (in electron volts) required to remove the electron from the electron donor ϕ_2^-, and a_0 corrects for the finite radii of ϕ_2^- and ϕ_3Et (a_0 is taken to be 5 Å).

Because the tunneling rate changes by a factor of 10 for each 1.8-Å change in distance, the electron will be transferred from ϕ_2^- to the nearest ϕ_3Et (*3*). If ϕ_2^- is randomly distributed relative to ϕ_3Et, then the fraction of the ϕ_2^- which survives reaction is (*3*)

$$P = \exp(-2.51 \times 10^{-3}\, a^3\, M) \quad (3)$$

where M is the molar concentration, and a increases with time according to Eq. 2. For the calculated curves given in Fig. 1, B was taken to be 1.6 ev, which is the photon energy necessary to photodetach electrons from ϕ_2^- in a hydrocarbon matrix (*3*).

An efficiency factor was introduced as an adjustable parameter since the observed reactions were slightly slower than the calculation. This factor could be considered to represent the slowing of the reaction as a result of Franck-Condon restrictions. This efficiency factor, taken to be $10^{-1.5}$, affected the calculated curves by simply translating them 1.5 units along the log t axis in Fig. 1. This efficiency factor, the only adjustable parameter in the calculation, could have been omitted and a similar fit to the data obtained, if the binding energy were treated as an adjustable parameter.

The kinetics of the observed reactions are very unusual but are in accord with the predictions of a simple model of electron tunneling. The frozen ethanol matrix is known to trap reactive species such as solvated electrons indefinitely (for days at least). This and the unusual kinetics tend to rule out any diffusion mechanism. At the ϕ_3Et concentrations of 0.10M, 0.03M, and 0.01M, the average distances from a ϕ_2^- to the *nearest* ϕ_3Et are 14, 21, and 30 Å, respectively, on the assumption of a random distribution. These and other results (*1–3, 5, 6*) point strongly toward a reaction mechanism in which electrons tunnel through tens of angstroms of inert matrix.

The simple model applied here works reasonably well, but why it works is not known. An appropriate theory must treat not only the electronic and nuclear states of the electron donor and acceptor molecules but also those of the intervening solvent. Approaches to at least part of this problem are being worked out in theories which describe electron transfer reactions in solution as tunneling processes by the use of modern radiationless transition theory (*10*).

JOHN R. MILLER

Chemistry Division, Argonne National Laboratory, Argonne, Illinois 60439

References and Notes

1. B. G. Ershov and E. L. Tseitlin, *Khim. Vys. Energ.* **4**, 186 (19→ F. Kieffer, C. Meyer, J. Rigant, *Chem. Phys. Lett.* **11**, 359 (1971); K. I. Zamaraev, R. F. Khairutidov, A. I. Mikhailov, V. I. Goldanskii, *Dokl. Akad. Nauk SSSR* **199**, 640 (1971); → J. Kroh and C. Stradowski, *Int. J. Radiat. Phys. Chem.* **5**, 243 (1973).
2. A. I. Mikhailov, *Dokl. Akad. Nauk SSSR* **197**, 136 (1971). → J. R. Miller, *J. Chem. Phys.* **56**, 5173 (1971).
4. A. Habersbergerova, *Radiat. Res. Rev.* **4**, 123 (19→ N. Christodouleas and W. Hamill, *J. Am. Chem. Soc.* **86**, 5413 (1964).
5. D. DeVault and B. Chance, *Biophys. J.* **6**, 825 (19→ D. DeVault, J. Parkes, B. Chance, *Nature (Lond.)* **215**, 642 (19→ J. D. McElroy, D. C. Mauzerall, G. Feher, *Biochim. Biophys. Acta* **333**, 261 (1974).
→ J. Miller, *Chem. Phys. Lett.* **22**, 180 (1973).
7. A. K. Pikaev, *The Solvated Electron in Radiation Chemistry* [Israel Program for Scientific Translations, Jerusalem (available from the U.S. National Technical Information Service, Springfield, Va.), 1973].
8. R. M. Hochstrasser and M. Kasha, *Photochem. Photobiol.* **3**, 317 (1964).
9. R. Foster, *Organic Charge-Transfer Complexes* (Academic Press, New York, 1969), p. 297.
10. For recent examples with several references, → S. F. Fisher, *Chem. Phys.* **5**, 183 (19→ N. R. Kestner, J. Logan, J. Jortner, *J. Phys. Chem.* **78**, 2148 (1974).
11. Based on work performed under the auspices of the U.S. Atomic Energy Commission.

25 September 1974; revised 21 March 1975

Hammondia hammondi: A New Coccidium of Cats Producing Cysts in Muscle of Other Mammals

Abstract. *Predominant muscle parasitism, and an obligatory two-host cycle (cat-mouse-cat), distinguishes an otherwise similar organism from* Toxoplasma. *The presence of multiplicative stages in the cat gut separate it from* Sarcocystis. *Antibody that cross reacts with* Toxoplasma *antigen is developed in mice and other experimental intermediary hosts, but not in cats, the final host. Recognition of the two-host cycle is essential for the experimental isolation and transmission of the parasite, and for prevention of the infection.*

We isolated an organism from a cat (CR-4) which showed similarities to both *Toxoplasma* and *Sarcocystis*, but which was significantly different from either. Oocysts resembling those of *Toxoplasma* appeared in the feces of an adult feral cat that had been injected with an immunosuppressive corticosteroid. Mice injected with oocysts developed low titers of *Toxoplasma* antibody without evidence of lesions in viscera and brain, but with cysts in skeletal muscle. Although the cysts contained organisms resembling *Toxoplasma*, they were not infectious to other mice. Cysts were infectious to cats which, however, failed to develop antibody to *Toxoplasma*.

We made a systematic comparison with the M-7741 strain of *Toxoplasma*, using techniques in mice and cats as described (*1*).

Oocysts shed by cats were subspherical to spherical, measuring 10.6 by 11.4 μm (10.5 to 12.5 by 11.2 to 13.2 μm). The oocyst wall was colorless, about 0.5 μm in thickness, and consisted of two layers. A micropyle and polar granules were absent. The sporont was uniformly granular and filled about 90 percent of the optical cross section of the oocyst.

Sporulation of oocysts was complete at 72 hours at 20° to 23°C, with two sporocysts containing four sporozoites each. The sporulated oocyst was subspherical to ellipsoidal, measuring 10.6 by 13.2 μm (10.0 to 10.7 by 12.6 to 13.8 μm). There was no oocyst residuum (Fig. 1A).

Sporocysts measured 6.5 by 9.8 μm (6.0 to 7.5 by 8.0 to 10.7 μm). There was no Stieda body. The sporocyst residuum consisted of granules, either dispersed or compact, near the center of the sporocyst. The sporozoites were elongate and slightly curved, measuring approximately 2 by 7 μm; the nucleus was centrally placed.

In mice infected with sporulated oocysts, organisms multiplied initially in the gut wall and mesenteric lymph nodes. After 11 to 16 days, cysts were seen in sections of skeletal muscle and cardiac muscle; after 20 to 48 days in fresh spreads of abdominal wall and diaphragm (Fig. 1, B and C). This was accompanied by necrosis, myositis, and myocarditis.

Cysts gradually increased in size to about 90 by 340 μm and persisted for at least 500 days in the skeletal muscle of mice. Cysts in heart muscle were few and rarely exceeded 30 μm in length. Cysts in brain tissue were rare, spherical in configuration, and measured up to 70 μm in diameter.

Bradyzoites, slowly multiplying organisms within the cysts, were slender, measuring about 2 by 7 μm, and resembled *Toxoplasma*. They differed from the broad and stubby bradyzoites of *Sarcocystis*.

In cats infected with skeletal muscle of